Antiferromagnetism in LiFePO₄*

By R. P. Santoro† and R. E. Newnham‡

Electrical Engineering Department, Massachusetts Institute of Technology, Cambridge, Massachusetts, U.S.A.

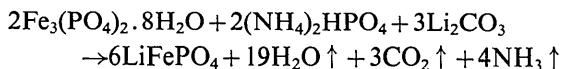The magnetic structure of LiFePO₄ has been determined from neutron diffraction data. Magnetic susceptibility measurements on polycrystalline material gave $p_{\text{eff}} = 5.45\mu_B$, $\theta = 88°K$, and $T_N = 50°K$. Below the Néel temperature, the Fe^{2+} spins align in an antiferromagnetic array collinear with **b**. The magnetic space group is *Pnma'*. LiFePO₄ is isostructural with olivine; the magnetic properties of the transition-metal olivines are summarized.

Introduction

Triphylite and lithiophilite, the lithium orthophosphates of divalent iron and manganese, form a solid solution series isomorphous with olivine. They occur in pegmatite granites in association with other phosphates, tourmaline and beryl. The magnetic properties of LiFePO₄ and LiMnPO₄ are reported in this paper.

Synthetic LiFePO₄ was prepared from the solid state reaction

$$2Fe_3(PO_4)_2 . 8H_2O + 2(NH_4)_2HPO_4 + 3Li_2CO_3$$
$$\rightarrow 6LiFePO_4 + 19H_2O \uparrow + 3CO_2 \uparrow + 4NH_3 \uparrow$$

After mixing in alcohol, the constituents were heated to 800°C for 48 hours in pre-purified nitrogen; the sample was surrounded by iron powder during the firing operation as a precaution against oxidation.

LiMnPO₄ was synthesized by the flux-melt technique of Zambonini & Malossi (1931).

The X-ray diffraction pattern of polycrystalline LiFePO₄ (Table 1) was recorded on a diffractometer with filtered Fe *K*α radiation. When indexed on the orthorhombic unit cell of olivine, the observed interplanar spacings gave $a = 10.314 \pm 0.010$, $b = 5.997 \pm 0.004$, and $c = 4.686 \pm 0.003$ Å. The space group is *Pnma* with $Z = 4$. Some authors prefer a setting corresponding to space group *Pbnm*. Intensities were calculated for three cation distributions: (i) Li in inversion sites as in LiMnPO₄ and Fe in mirror positions, (ii) Fe in inversion sites as in CaFeSiO₄ and Li in mirror positions, and (iii) random occupation of the two sites as in (Mg,Fe)₂SiO₄. Model (i) was in excellent agreement with experiment (Table 1), verifying the arrangement proposed by Destenay (1950). Models (ii) and (iii) gave agreement indices (*R*) of 1·17 and 0·71 compared with 0·15 for the correct structure. LiFePO₄ is therefore isomorphous with LiMnPO₄ (Geller & Durand, 1960) and other LiXPO₄ compounds (Newnham & Redman, 1965).

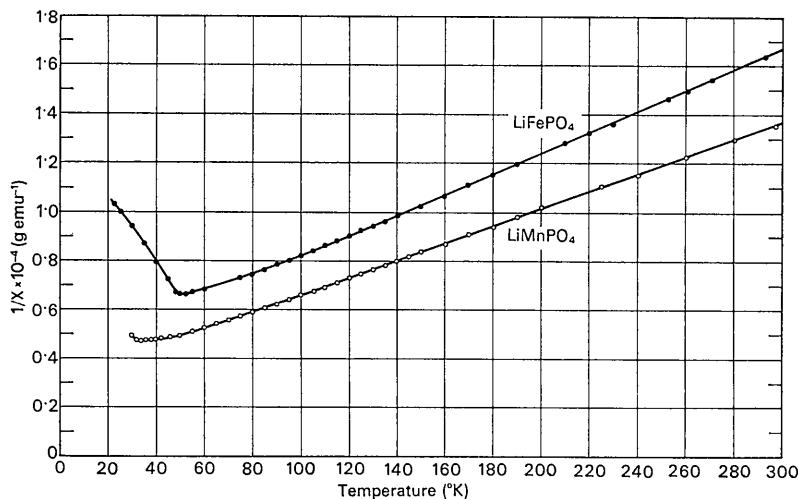The magnetic susceptibilities of LiFePO₄ and LiMnPO₄ ceramics were measured from 20°K to room

Fig. 1. Reciprocal magnetic susceptibilities of polycrystalline LiFePO₄ and LiMnPO₄.

temperature. The experiments were performed on a vibrating-sample magnetometer (Foner, 1959) using a field of 10kG; no field dependence of the susceptibility was observed. When plotted as a function of temperature (Fig. 1), the reciprocal susceptibility of LiFePO$_4$ shows a minimum at $50 \pm 2\,°$K, indicating a paramagnetic–antiferromagnetic phase transition. Data collected in the paramagnetic region show typical Curie–Weiss law behavior with $p_{eff} = 5·45 \pm 0·10\mu_B$ and $\theta = 88 \pm 5\,°$K. For LiMnPO$_4$, $T_N = 35 \pm 2\,°$K, $p_{eff} = 5·95 \pm 0·12\mu_B$ and $\theta = 85 \pm 5\,°$K. Previous susceptibility measurements on lithiophilite (Mays, 1963) differ by about 10%, though the transition temperatures agree. Bozorth & Kramer (1959) obtained comparable results on a mineral specimen with composition LiMn$_{0·7}$Fe$_{0·3}$PO$_4$; their measurements gave $p_{eff} = 6·1\mu_B$, $\theta = 80\,°$K and $T_N = 42\,°$K.

Neutron diffraction powder patterns of LiFePO$_4$ were taken above and below the transition temperature at 300 and 9 °K. Observed nuclear and magnetic intensities are listed in Table 1. Nuclear intensities calculated from the refined lithiophilite coordinates (Geller & Durand, 1960) gave an R value of 0·10, confirming the X-ray result. The magnetic reflections can be indexed on the chemical unit cell, and the low-temperature spin structure was determined by trial and error.

In the triphylite structure the Fe^{2+} ions occupy equi-point $4(c)$ at coordinates $0·28,\frac{1}{4},0·98$; $0·72,\frac{3}{4},0·02$; $0·22,\frac{3}{4},0·48$; $0·78,\frac{1}{4},0·52$. The spin vectors associated with these positions are labeled S$_5$, S$_6$, S$_7$ and S$_8$, respectively (S$_1$ through S$_4$ are reserved for the inversion sites, which are occupied by non-magnetic lithium ions in LiFePO$_4$). Three antiferromagnetic arrangements must be considered:

$$G = S_5 - S_6 + S_7 - S_8$$
$$A = S_5 - S_6 - S_7 + S_8$$
$$C = S_5 + S_6 - S_7 - S_8$$

Ferro- and ferri-magnetic structures are ruled out by the susceptibility data. G consists of alternating ferromagnetic planes perpendicular to **a**; it has not been observed in the transition-metal olivine family. A is the configuration observed in LiMnPO$_4$ (Mays, 1963) and C occurs in the Co$_2$SiO$_4$ group (Nomura, Santoro, Fang & Newnham, 1964).

As shown in Table 1, the two most intense magnetic reflections observed for LiFePO$_4$ are 101 and 210. Both structure factors are identically zero for arrangements G and C, eliminating them from further consideration. Only the spin direction associated with A remains to be determined. With spins collinear with **a** or **c**, a large 010 reflection is predicted; experimentally 010 is not observed and we conclude that A_y is the dominant

Table 1. *Comparison of observed and calculated intensities for the* LiFePO$_4$ *X-ray and neutron diffraction powder patterns*

hkl	d	X-ray I_c	I_o	Nuclear I_c	I_o	Magnetic I_c	I_o
100	10·314	0	<10	0	<20	0	<20
010	5·997	0	<10	0	<20	0	<20
110	5·184	0	<10	0	<20	0	<20
200	5·157	84	110	136	171	41	40
001	4·686	0	<10	0	<20	7	<20
101	4·266	229	300	468	463	323	329
210	3·910	94	95	163	166	134	137
011	3·693	39	33	66	116	0	<20
111	3·477	239 }	287	233 }	258	10 }	<20
201	3·469	62 }		78 }		5 }	
300	3·438	0	<10	0	<20	0	<20
211	3·002	48 }	260	67 }	422	1 }	<20
020	2·999	248 }		377 }		0 }	
310	2·983	0	<10	0 }		0 }	
120	2·879	0	<10	0	<20	0	<20
301	2·772	94	100	53	74	66	79
220	2·592	4	<10	60 }	107	3 }	37
400	2·578	0	<10	46 }		22 }	
021	2·526	0	<10	0 }	350	1 }	24
311	2·516	354	350	404 }		39 }	
121	2·453	114	90	67	64	43	31
410	2·369	76	53	59 }	283*	25 }	44*
002	2·343	1	<10	95 }		0 }	
102	2·285	43	46	77 }		1 }	
221	2·268	44	60	442 }	920	1 }	<20
320	2·260	0 }	55	0 }		0 }	
401	2·259	53 }		343 }		1 }	
012	2·183	0	<10	0	<20	23 }	19
112	2·135	32 }	62	77 }	183	8 }	24
202	2·133	42 }		127 }		6 }	
411	2·114	1	<10	5 }		1 }	

* 111 reflection from the aluminum sample holder superimposed.

mode. Group theoretical arguments applied to other structures in this space group (Bertaut, 1963) show that A_y is a unique mode with no mixing. In A_y, S_5 and S_8 are parallel to $\mathbf{b}$ and antiparallel to S_6 and S_7. The magnetic space group of LiFePO$_4$ is $Pnma'$. Intensity calculations (Table 1) based on this structure gave generally good agreement and an R value of 0·11. An atomic moment $gS = 3·84\mu_B$ was computed from the 101 and 210 intensities.

The LiFePO$_4$ magnetic structure (Fig. 2) is identical with that of LiCoPO$_4$ and differs only in spin direction from those of LiMnPO$_4$ and LiNiPO$_4$. Magnetic properties of these and other transition-metal olivines are summarized in Table 2. Olivine is a hexagonal close-packed analog to cubic close-packed spinel. Both are M$_2$XO$_4$ compounds with tetrahedral X cations and octahedral M cations coordinated to a close-packed framework of oxygens. Olivine crystallizes in preference to spinel for certain small X ions, such as Be^{2+}, B^{3+}, Si^{4+}, P^{5+}, and occasionally Ge^{4+}. Transition-metal atoms occupy the distorted octahedral sites, half of which possess inversion symmetry and the remainder lie on mirror planes. The two sites differ in size as well as symmetry, often giving rise to ordering. In contrast to the spinel–ferrite family, the magnetic properties of the transition-metal olivines have received little attention. The compounds listed in Table 2 are all antiferromagnetic at low temperatures, with several different magnetic structures.

In Cr$_2$BeO$_4$ and the orthosilicates of divalent manganese, iron, cobalt and nickel, both octahedral sites are filled by transition elements. Of all the olivines, the collinear magnetic structure of Co$_2$SiO$_4$ is perhaps the easiest to understand. If, as in most transition-metal oxides, an antiferromagnetic superexchange mechanism dominates, the geometry of the Co–O–Co interactions

leads directly to the observed spin array. Manganese and iron orthosilicate have similar structures just below T_N, but canting occurs in the inversion site spins at lower temperatures. The inversion positions are closely spaced along $\mathbf{b}$ and overlapping $3d$ wave functions lead to an antiferromagnetic direct interaction, causing canting. Ni$_2$SiO$_4$ and Cr$_2$BeO$_4$ adopt more complicated magnetic structures. The magnetic reflections of nickel orthosilicate can be indexed on a $2\mathbf{a} \times \mathbf{b} \times 2\mathbf{c}$ superlattice cell containing 32 spins. Cr$_2$BeO$_4$ has a complex neutron diffraction pattern which may lead to a spiral configuration, similar to those observed in chromium-bearing spinels.

Additional information regarding the direct exchange interactions is obtained from the transition-metal calcium orthosilicates (Table 2). Divalent Mn,
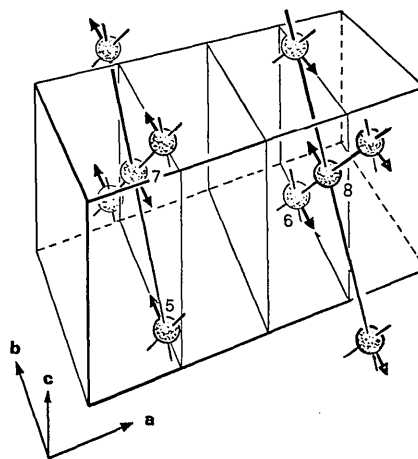

Fig. 2. Magnetic structure of LiFePO$_4$. Only the iron positions are shown.

Table 2. *Magnetic properties of the transition-metal olivines*

Compound	$p_{eff}(\mu_B)$	θ (°K)	T_N (°K)	Magnetic structure	Reference
Cr$_2$BeO$_4$	3·24	13	28	Complex	Santoro & Newnham (1964)
Mn$_2$SiO$_4$	5·87	163			Kondo & Miyahara (1963)
	5·86	163	50	Collinear 13–50°K	Santoro, Newnham & Nomura (1966)
				Canted below 13°K	Cox, Frazer, Almodovar & Kay (1965)
Fe$_2$SiO$_4$	6·05	150			Kondo & Miyahara (1963)
	6·03	126	65	Collinear 23–65°K	Santoro, Newnham & Nomura (1966)
				Canted below 23°K	Cox, Frazer, Almodovar & Kay (1965)
			65		Kelley (1941)
Co$_2$SiO$_4$	4·6	15			Kondo & Miyahara (1963)
	5·01	60			Goodgame & Cotton (1961)
	5·09	65	49	Collinear	Nomura, Santoro, Fang & Newnham (1964)
Ni$_2$SiO$_4$	3·04	−14			Kondo & Miyahara (1963)
	3·15	7	34	Supercell	Newnham, Santoro, Fang & Nomura (1965)
CaMnSiO$_4$	5·77	26	9	Collinear	Caron, Santoro & Newnham (1965)
CaFeSiO$_4$	5·7	12	<8	Paramagnetic	Newnham, Caron & Santoro (1966)
CaCoSiO$_4$	4·8	1	16	Supercell	Newnham, Caron & Santoro (1966)
LiMnPO$_4$	5·95	85	35	Collinear	Mays (1963); Present paper
LiFePO$_4$	5·45	88	50	Collinear	Present paper
LiCoPO$_4$	5·7	90	23	Collinear	Santoro, Segal & Newnham (1966)
LiNiPO$_4$	3·35	79	23	Collinear	Santoro, Segal & Newnham (1966)

Fe or Co occupies the inversion centers with calcium in mirror plane positions, isostructural with monticellite ($CaMgSiO_4$). Attempts to synthesize $CaNiSiO_4$ proved unsuccessful. In $CaMnSiO_4$, the manganese moments align in antiferromagnetic chains along **b** with spin directions collinear with **c**. The cobalt salt has a large magnetic cell similar to Ni_2SiO_4, but systematic absences suggest a ferromagnetic direct interaction. $CaFeSiO_4$ remains paramagnetic to low temperatures.

Only superexchange interactions occur in the lithiophilite–triphylite group where the transition-metal ions are partially replaced by the smaller Li^+ ion. As mentioned previously, the $LiMPO_4$ (M = Mn, Fe, Co, Ni) compounds possess similar magnetic structures. M–O–M superexchange interactions give rise to antiferromagnetic puckered-planes orthogonal to **a**. There are no direct or superexchange linkages between these planes, and it is necessary to postulate long-range interactions, such as the Mn–O–P–O–Mn triple exchange suggested by Mays (1963).

In $LiMnPO_4$ and Mn_2SiO_4 the spins align along **a**, the direction minimizing the magnetic dipole energy. **b** is the preferred direction for the iron and cobalt compounds, in which spin-orbit and crystal field interactions are often decisive. The spin direction of the magnetically ordered lithiophilite–triphylite series must depend on composition since the magnetic structures of the end members differ. Susceptibility measurements on $LiMn_{0.7}Fe_{0.3}PO_4$ single crystals (Bozorth & Kramer, 1959) specify **b** as the spin direction, like $LiFePO_4$. The change in spin direction therefore takes place in manganese-rich compositions near $LiMnPO_4$.

References

BERTAUT, E. F. (1963). *Magnetism,* Vol. III, 157. (G. T. Rado & H. Suhl, Editors). New York & London: Academic Press.
BOZORTH, R. M. & KRAMER, V. (1959). *J. Phys. Radium,* **20**, 393.
CARON, L. G., SANTORO, R. P. & NEWNHAM, R. E. (1965). *J. Phys. Chem. Solids,* **26**, 927.
COX, D. E., FRAZER, B. C., ALMODOVAR, I. & KAY, M. I. (1965). Abstracts A.C.A. Annual Meeting, Gatlinburg, Tenn. p. 47.
DESTENAY, D. (1950). *Mém. Soc. Roy. Sci. Liège,* **10**, 5.
FONER, S. (1959). *Rev. Sci. Instrum.* **30**, 548.
GELLER, S. & DURAND, J. L. (1960). *Acta Cryst.* **13**, 325.
GOODGAME, M. & COTTON, F. A. (1961). *J. Chem. Phys.* **65**, 791.
KELLEY, K. K. (1941). *J. Amer. Chem. Soc.* **63**, 2750.
KONDO, H. & MIYAHARA, S. (1963). *J. Phys. Soc., Japan,* **18**, 305.
MAYS, J. M. (1963). *Phys. Rev.* **131**, 38.
NEWNHAM, R. E., CARON, L. G. & SANTORO, R. P. (1966). *J. Amer. Ceram. Soc.* In the press.
NEWNHAM, R. E. & REDMAN, M. J. (1965). *J. Amer. Ceram. Soc.* **48**, 547.
NEWNHAM, R., SANTORO, R., FANG, J. & NOMURA, S. (1965). *Acta Cryst.* **19**, 147.
NOMURA, S., SANTORO, R., FANG, J. & NEWNHAM, R. (1964). *J. Phys. Chem. Solids,* **25**, 901.
SANTORO, R. P. & NEWNHAM, R. E. (1964). *J. Amer. Ceram. Soc.* **47**, 491.
SANTORO, R. P., NEWNHAM, R. E. & NOMURA, S. (1966). *J. Phys. Chem. Solids.* **27**, 655.
SANTORO, R. P., SEGAL, D. J. & NEWNHAM, R. E. (1966). *J. Phys. Chem. Solids.* **27**, 1192.
ZAMBONINI, F. & MALOSSI, L. (1931). *Z. Kristallogr.* **80**, 442.

Five New Zinc Sulphide Polytypes: 10L (8 2); 14L (5 4 2 3); 24L (5 3)₃; 26L (17 4 2 3) and 28L (9 5 5 9)

BY O. BRAFMAN, E. ALEXANDER AND I. T. STEINBERGER

Department of Physics, The Hebrew University, Jerusalem, Israel

The layer sequences of some ZnS polytypes have been determined by comparing observed X-ray reflexion intensities with those calculated by a computer. It is demonstrated that birefringence measurements facilitate these determinations, since the number of elements of the Zhdanov symbol can be known from measuring the degree of the birefringence. Differences of polytypism in SiC and ZnS are discussed briefly.

Introduction

It has been known (Frondel & Palache, 1950), that both natural and artificially grown ZnS crystals often exhibit polytypism. Still, very little is known about polytypism in ZnS, since even in the cases where the existence of a polytype has been reported, usually only the periodicity of the structure is given and the actual stacking sequence is missing. The only exceptions are 6L [six-layer periodicity, (3 3)], 15L (3 2)₃ (Frondel & Palache, 1950), 8L (4 4) and 10L (5 5) (Evans & McKnight, 1959), the symbols in parentheses denoting